Journal of the Optical Society of America B
OPTICAL PHYSICS

Review of recent progress on single-frequency fiber lasers

Shijie Fu,[1] Wei Shi,[1,2,*] Yan Feng,[3,6] Lei Zhang,[3] Zhongmin Yang,[4] Shanhui Xu,[4,7] Xiushan Zhu,[5] R. A. Norwood,[5] and N. Peyghambarian[5]

[1]College of Precision Instrument and Optoelectronics Engineering, Tianjin University, Tianjin 300072, China
[2]Tianjin Institute of Modern Laser & Optics Technology, Tianjin 300384, China
[3]Shanghai Institute of Optics and Fine Mechanics, Chinese Academy of Sciences, and Shanghai Key Laboratory of Solid State Laser and Application, Shanghai 201800, China
[4]State Key Laboratory of Luminescent Materials and Devices and Institute of Optical Communication Materials, South China University of Technology, Guangzhou 510640, China
[5]College of Optical Sciences, University of Arizona, 1630 E. University Blvd., Tucson, Arizona 85721, USA
[6]e-mail: feng@siom.ac.cn
[7]e-mail: flxshy@scut.edu.cn
*Corresponding author: shiwei@tju.edu.cn

Received 30 September 2016; revised 9 January 2017; accepted 19 January 2017; posted 19 January 2017 (Doc. ID 277898); published 15 February 2017

Single-frequency fiber lasers have drawn intense attention for their extensive applications from high-resolution spectroscopy and gravitational wave detection to materials processing due to the outstanding properties of low noise, narrow linewidth, and the resulting long coherence length. In this paper, the recent advances of single-frequency fiber oscillators and amplifiers are briefly reviewed in the broad wavelength region of 1–3 μm. Performance improvements in laser noise and linewidth are addressed with the newly developed physical mechanisms. The solution to achieving higher power/energy is also discussed, accompanied by the start-of-the-art results achieved to date.

OCIS codes: (140.3510) Lasers, fiber; (140.3570) Lasers, single-mode; (060.2320) Fiber optics amplifiers and oscillators; (140.3070) Infrared and far-infrared lasers.

https://doi.org/10.1364/JOSAB.34.000A49

1. INTRODUCTION

Since the first demonstration by Snitzer in 1964 [1], fiber lasers have experienced extensive research and development over the past five decades. As a powerful competitor, fiber lasers exhibit many advantages over bulk solid state lasers, which motivate the related scientific study and attract great commercial interest [2]. The unique geometry of the fiber gain medium allows for efficient heat dissipation due to the large surface area to active volume ratio. This makes thermal management easily attainable and benefits the laser power scaling. The confinement of laser radiation in the fiber waveguide structure ensures excellent output beam quality. Thermally induced mode distortion, commonly observed in traditional solid state lasers, can be significantly alleviated if accompanied by a specific physical design of the fiber. The all-fiberized structure design eliminates the need for complicated alignment of free-space optical components and thus simplifies the laser architecture, contributing to the compactness and ruggedness of the fiber laser. The outstanding characteristics aforementioned enable a wide range of applications of fiber lasers in scientific research, industrial processing, defense and security, and so on.

Over the past 50 years, especially over the past decade, with the development of fiber material and drawing technology, fiber component fabrication, and high-brightness pumping diodes, the performance of fiber lasers has been improved in various aspects. A broad selection of emission wavelengths have been realized in the range from ultraviolet, visible, near-infrared to mid-infrared [3–7]. In continuous-wave fiber lasers, an output power of 10 kW with nearly diffraction-limited beam quality has been achieved from a single large-mode-area (LMA) fiber in 2009 [8]. Pulse energy up to 26 mJ has been obtained from a single-mode Q-switched nanosecond fiber laser [9]. For ultrashort pulse fiber technology, few-cycle light with pulse duration shorter than 10 fs has been produced in fiber lasers [10,11]. All of these achievements enrich the applications for fiber lasers and drive their practical deployment. On the other hand, with the demand increase of some practical applications, such as high-precision metrology, gravitational wave detection, and coherent LIDAR, fiber lasers operating with narrow linewidths are urgently required [12–15]. Therefore, single-frequency fiber lasers, which means lasers running with single-longitudinal-mode, have attracted intense attention and have been broadly researched recently. Low-noise, single-frequency sources with linewidths as narrow as several kilohertz or even subkilohertz were developed in different configurations. So far, while some specific aspects of single-frequency fiber lasers, such as heavily rare-earth-doped special glass fibers and power scaling of single-frequency fiber lasers, have been addressed in the literature [16–18], a formal review on the development of single-frequency fiber lasers has not yet been conducted.

In this paper, we will review the major significant progress made to date for single-frequency fiber lasers. The structure of the paper is arranged as follows. In Section 2, we introduce the configurations of single-frequency fiber oscillators and current achievements in different wavelength regimes—as best exemplified by progress in single-frequency distributed Bragg reflector (DBR) fiber lasers, which is the preferred laser configuration by virtue of its simplicity, compactness, and robustness. In particular, the new extended wavelengths for single-frequency lasing are presented with more information. In Section 3, we summarize the newly developed experimental techniques and physical mechanisms to realize performance improvement of single-frequency fiber lasers with respect to ultralow noise and ultranarrow linewidth. The state-of-the-art results on high-power single-frequency fiber amplifiers in both continuous-wave (CW) and pulsed mode are reviewed in Section 4. Finally, we give a summary to this paper in Section 5.

2. PROGRESS ON SINGLE-FREQUENCY FIBER OSCILLATORS

As the study on the single-frequency fiber lasers develops, different configurations have been implemented to demonstrate single-longitudinal-mode operation. In general, they can be summarized as distributed feedback (DFB) fiber lasers [19–21], DBR fiber lasers [22–24], and ring cavity fiber lasers embedded with narrow-bandwidth filters [25–27]. A DFB fiber laser is composed of a piece of fiber Bragg grating (FBG) written directly in the active fiber, which introduces a phase change in the middle of the grating area. The resulting structure functions as an ultranarrow spectral filter to achieve single-mode oscillation. Nevertheless, the power a single-frequency DFB fiber laser can provide is very limited. In addition to the short cavity length and low signal gain, the thermal effects in the phase-shifted FBG-based cavity are serious at high pump powers, which can change the refractive index and then dephase the grating [28]. The DBR single-frequency fiber laser is another typical linear cavity design with the structure shown in Fig. 1. The laser cavity combines a pair of narrowband FBGs with a short piece of rare-earth-doped fiber, which shows attractive properties in terms of simplicity and compactness. For single-frequency operation, the length of the active fiber is usually limited to several centimeters, requiring that a high gain coefficient can be provided [29]. To enlarge the active fiber length for higher laser power, ring cavity fiber lasers embedded with narrowband filters were developed. Among them, the FBG-based Fabry–Perot etalon [30], saturable absorber [31],

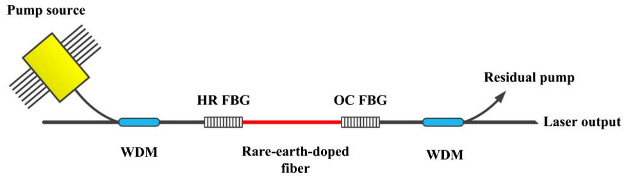

Fig. 1. Typical schematic of a single-frequency DBR fiber laser. HR-FBG, high-reflection FBG; PR-FBG, partial-reflection FBG.

and short subcavity [32] have been proposed as approaches to obtaining single-frequency lasing in a ring cavity. However, in each case, additional loss is also introduced to the laser cavity and the complexity of the laser system has been increased. Overall, DBR fiber lasers are preferred in the development of single-frequency fiber lasers because of their compactness and robustness. Therefore, in this part, we mainly reviewed the progress of the single-frequency fiber laser in the DBR scheme.

Although the first single-frequency DBR fiber laser was demonstrated as early as 1988 [22], the laser output power was initially limited to several milliwatts. The heart of the fiber laser—active fiber—is commonly based on the silica host glass, whose capability to be doped with high concentrations of rare-earth ions was limited by its intrinsic structure. More recently, the rare-earth-doped soft glass fibers, such as phosphate glass fiber [33] and germanate glass fiber [34], were developed. The properties, such as doping concentration, absorption and emission cross sections, and gain spectra, have been investigated and systematically characterized [35–40]. Figure 2 is a summary of the typical spectra for Er^{3+}, Yb^{3+}, and Tm^{3+} in different host compositions. Due to the high rare-earth ion solubility in these hosts, such soft glass fibers exhibit extremely high optical gain per unit length of generally several decibels per centimeter [41–44]. This enables efficient operation of short-length single-frequency fiber lasers, especially compact DBR fiber lasers, where the output power can be up to hundreds of milliwatts or even at the watt level. In Table 1, we summarize the output features of the single-frequency fiber laser demonstrated with rare-earth-doped soft glass fibers in the regimes of 1, 1.5, and 2 μm [24,28,35,45–57]. Here we list the primary experimental results on single-frequency fiber lasers demonstrated with different rare-earth-doped soft glass fibers; the table is organized according to chronological order for different operating regions.

In the 1 μm regime, a high-power single-frequency fiber laser is generally achieved with Yb^{3+}-doped phosphate glass fibers, which allow for doping concentrations of > 10 wt.% Yb^{3+} [58,59]. It is much higher than the concentrations in silica fiber (of the order of 1–2 wt. %) [60]. For the report in Ref. [46], up to 15.2 wt. % Yb^{3+} were doped uniformly in the core region of phosphate glass fiber to achieve a net gain coefficient of ~5.7 dB/cm. The peak absorption coefficient of the fiber core glass is 10.7 cm^{-1} at 976 nm. Such a large absorption coefficient allows efficient absorption of the pump light within a few centimeters and can generate hundreds of milliwatts of output power without the need for an external optical amplifier. With only 0.8 cm Yb^{3+}-doped phosphate fiber, a high-efficiency single-frequency fiber was achieved with so far the highest output power of more than 400 mW.

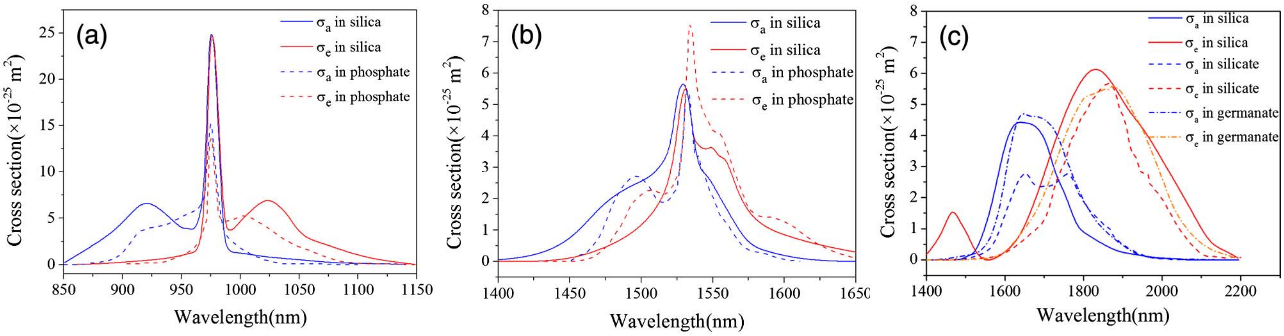

Fig. 2. Typical absorption and emission spectra of (a) Yb^{3+} in silica and phosphate, (b) Er^{3+} in silica and phosphate, and (c) Tm^{3+} in silica, silicate, and germanate glass. The data of the spectra were based on the published literature [35–40].

Table 1. Progress of Single-Frequency Fiber Oscillators Based on Heavily Rare-Earth-Doped Soft Glass Fibers

Fiber Type [Reference]	λ_{pump} (nm)	λ_{laser} (nm)	Output Power (mW)	Slope Efficiency (%)	Rare-Earth-Doped Concentration or Gain Coefficient	Laser Linewidth (kHz)	Gain Length (cm)
Yb^{3+}-doped phosphate [45]	976	1064	>200	31	2 dB/cm	3	1.5
Yb^{3+}-doped phosphate [46]	976	1064	>400	72.7	15.2 wt. % Yb^{3+} (5.7 dB/cm)	<7	0.8
Yb^{3+}-doped phosphate [35]	915	976	100	25	6 wt. % Yb_2O_3	<3	2
Yb^{3+}-doped phosphate [47]	976	1083	100	29.6	18.3 wt. % Yb^{3+}	<2	1.8
Yb^{3+}-doped phosphate [48]	976	1120	62	17.2	15.2 wt. % Yb^{3+}	5.7	3.1
Er^{3+}/Yb^{3+}-codoped phosphosilicate [28]	980	1535	58	12	—	500	1.5
Er^{3+}/Yb^{3+}-codoped phosphate [49]	976	1560	200	24.3	5 dB/cm	1.75	2
Er^{3+}/Yb^{3+}-codoped phosphate [24]	976	1550	1600	5	1.1×10^{26} Er^{3+}/m^3 and $8.6 \times 10^{26} Yb^{3+}/m^3$	—	5.5
Er^{3+}/Yb^{3+}-codoped phosphate [50]	976	1535	1900	11	1.1×10^{26} Er^{3+}/m^3 and 8.6×10^{26} Yb^{3+}/m^3	—	10
Er^{3+}/Yb^{3+}-codoped phosphate PCF [51]	976	1534	2300	12	1.6×10^{26} Er^{3+}/m^3 and 8.6×10^{26} Yb^{3+}/m^3	—	3.8
Er^{3+}/Yb^{3+}-codoped phosphate [52]	976	1535	306	30.9	5.2 dB/cm	1.6	2
Er^{3+}/Yb^{3+}-codoped phosphate [53]	975	1538	550	12	1 wt. % Er_2O_3 and 8 wt. % Yb_2O_3	<60	7
Tm^{3+}-doped germanate [54]	805	1893	50	35	5 wt. % Tm_2O_3	~3	2
Tm^{3+}-doped silicate [55]	1575	1950	40	20.4	5 wt.% Tm_2O_3	<3	2
Tm^{3+}-doped germanate [56]	1568	1950	100	24.7	~4.5×10^{26} Tm^{3+}/m^3	<6	2.1
Ho^{3+}-doped germanate [57]	1950	2053	60	—	3 wt.% Ho_2O_3	~10 s	2

In addition to the typical lasing wavelength at 1064 nm, single-frequency operation at other wavelengths has also been investigated [35,47,48] since Yb^{3+} can generate a broad range of laser emission from 970 to 1200 nm [61–63]. Narrow-linewidth laser sources below 1 μm are greatly demanded for nonlinear wavelength conversion to generate coherent blue light or even deep ultraviolet coherent sources. However, three-level lasing for a Yb^{3+}-doped fiber laser system is very difficult to achieve, especially for a short DBR fiber laser. For the Yb^{3+}-doped phosphate glass, a larger difference between the absorption and emission cross sections at wavelengths shorter than 1 μm, as shown in Fig. 2, makes it a potential medium for a laser at 976 nm. With 2 cm long Yb^{3+}-doped phosphate fiber, more than 100 mW of laser power can be obtained at 976 nm with a signal-to-noise ratio (SNR) of more than 50 dB [35]. No strong amplified spontaneous emission (ASE) or spurious lasing at longer wavelengths was observed benefiting from efficient energy extraction in this short-cavity scheme. On the other hand, with short-length Yb^{3+}-doped phosphate fiber, single-frequency operation was also investigated at longer wavelengths, such as 1083 nm [43] and 1120 nm [44]. Due to the relatively low emission cross section at these wavelengths, traditionally several meters of silica gain fiber would be employed to provide sufficient gain, which cannot be employed for a short-cavity single-frequency fiber laser. The high doping concentration of Yb^{3+}-doped phosphate fiber with up to 18.3 wt. % can efficiently compensate the low-emission cross section at lasing wavelengths. Even at 1120 nm, where a sharp drop in the emission cross section exists, around 62 mW of output power was achieved for stable single-longitudinal-mode lasing. More importantly, by optimizing the reflectivity of the output FBG and the length of gain fiber, the ASE at short wavelengths was well suppressed with an SNR larger than 67 dB.

In the 1.5 μm region, the first 100 mW single-frequency fiber laser was demonstrated in 2003 with a piece of highly Er^{3+}/Yb^{3+}-codoped phosphate fiber [23]. The core region of the active fiber was uniformly doped with 3 wt. % of Er^{3+} and 2 wt. % of Yb^{3+} [39]. With Yb^{3+} as the sensitizer, the absorbed energy can be efficiently transferred to Er^{3+}, and thus the cooperative upconversion and pair-induced quenching existing in high-Er^{3+}-concentration fiber are avoided. A gain coefficient up to 5 dB/cm was obtained at 1535 nm without ion clustering, based on which single-frequency operation was achieved with an output power of more than 120 mW. Further power scaling to the watt level for a single-frequency fiber laser was reached with the development of heavily Er^{3+}/Yb^{3+}-codoped double-cladding phosphate glass fiber and cladding pump technology. Output powers of 1.6 and 1.9 W were obtained successively with the short-cavity structure [24] and the twisted mode technique [50]. Furthermore, by using 3.8 cm of Er^{3+}/Yb^{3+}-codoped phosphate photonics crystal fiber (PCF) in a cladding pumping scheme [51], a single-mode, single-frequency laser with a record output power of 2.3 W was reported in 2006. However, the microstructured active fiber employed here made the fabrication process quite complicated since the laser cavity was composed of a dielectric coating and an FBG written in silica fiber. Due to the fusion splices and coupling losses between different fibers, propagation loss of the laser cavity reached 3.8 dB. In 2013, a monolithic, single-frequency all-phosphate glass fiber laser was presented to overcome these shortcomings [53]. The FBG pairs were inscribed directly into the active fiber with an ultrafast laser. By removing the fusion splices from the laser cavity in this way, the cavity loss can be reduced and the robustness can be improved. Moreover, the whole laser cavity is effective for power amplification. The lasing threshold was only 200 mW, even under cladding pumping, and the maximum output power of 550 mW was achieved with a slope efficiency of 12%. Although watt-level output power can be achieved from these high-gain double-cladding phosphate fibers, there are still some problems to be further solved—one is stability, for both the laser power and the single-longitudinal-mode operation, under high pump power. The disturbance of temperature in the fiber cavity may lead to the changes in laser cavity length and correspondingly the longitudinal-mode spacing [24].

Two micrometer fiber lasers have attracted broad research attention over the past several years for applications in laser surgery, environmental sensing, and coherent LIDAR [64–66]. Single-frequency fiber lasers in this regime have been implemented with Tm^{3+}-doped fibers [54–56,67–69] and Ho^{3+}-doped fibers [57,70]. Among them, the Tm^{3+}-doped germanate glass fiber laser exhibits highly efficient 2 μm operation, which was first investigated to achieve a single-frequency Tm^{3+}-doped fiber laser in 2007 [54]. A high slope efficiency of 35% benefitted from the high Tm_2O_3 doping concentration (5 wt. %) induced efficient cross-relaxation process and low phonon energy (900 cm^{-1}) in germanate glass. In 2015, Yang *et al.* improved the output power to more than 100 mW [56]. In addition, linearly polarized output was managed to facilitate its applications in gravitational wave detection, coherent polarization beam combination, and nonlinear frequency conversion. Recently, Wen *et al.* developed a highly Tm^{3+}-doped barium gallo-germanate (BGG) glass single-mode fiber with excellent properties of comparatively low phonon energy, high rare-earth solubility, and good mechanical characteristics. The Tm^{3+} doping concentration was improved to 7.6×10^{20} ions/cm^3, which is the reported highest level in Tm^{3+}-doped BGG fibers [71]. This can be a promising active medium for developing a high-power 2 μm single-frequency fiber laser.

Additionally, some other glass hosts, such as fluoride [72,73] and chalcogenide glass [74,75], have also been studied for expansion of the laser operation spectral region because of their broad transmission windows and low phonon energy. In particular, for the ZBLAN in fluoride glass, the small thermal dependence of optical properties and the ease of fiber drawing motivate its study as a laser medium [76]. One attempt for the single-frequency fiber laser is with the Ho^{3+}-doped ZBLAN fiber, which can generate efficient emission at 1.2 μm through the transition from excited state $^5I_6$ to ground state $^5I_8$, as shown in Fig. 3. The competitive 2.9 μm emission can be self-terminated due to the shorter lifetime of the $^5I_6$ state than the $^5I_7$ state. For practical applications, the cladding of the ZBLAN fiber was codoped with terbium to further suppress the 2.9 μm laser easily obtained in highly Ho^{3+}-doped ZBLAN fibers [77,78]. Single-frequency operation at 1.2 μm with the laser output power at about 10 mW was realized from a cavity composed of 22 mm long Ho^{3+}-doped ZBLAN fiber and a pair of silica-based FBGs [79]. Nevertheless, due to the large cavity loss as well as strong upconversion and excited-state absorption in highly Ho^{3+}-doped ZBLAN fiber, the efficiency of the fiber laser is only 3.8%.

The energy-level diagram in the inset of Fig. 3 also reveals that it can be a candidate for single-frequency lasing at 2.9 μm. However, an effort should be made to eliminate the potential self-termination due to the longer lifetime for the lower laser level $^5I_7$ for the 3 μm transition compared with the upper laser level $^5I_6$. Hudson *et al.* adopted the Ho^{3+}, Pr^{3+}-codoped fiber approach to efficiently reduce the lower laser lifetime (which reduces the lower laser level lifetime from 12 to <1 ms) and thus alleviate self-termination [72,80]. Narrow-linewidth feedback for the laser cavity was provided by an FBG inscribed directly in the fluoride fiber using femtosecond pulses and a point-by-point inscription technique [81]. A maximum output power of 11 mW was attained with a slope efficiency of 1.4%. It is a great demonstration to extend the operating wavelength

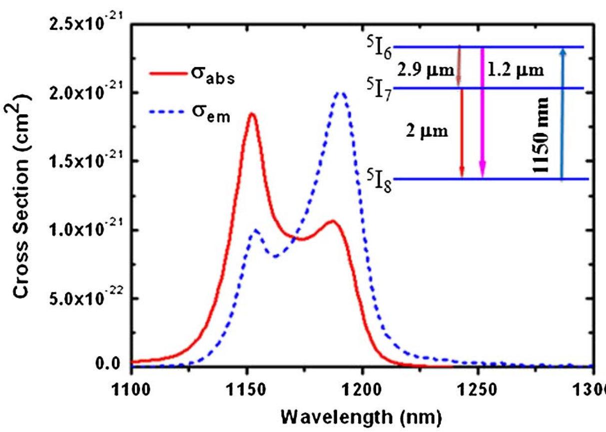

Fig. 3. Absorption and emission cross sections of Ho^{3+} ions in ZBLAN glass. (Inset: energy-level diagram and transitions related to the 1.2 μm emission.)

to the mid-IR, whereas the laser system is free-space coupled due to the fiber devices in the mid-IR wavelength not commercially available, and up to now the linewidth cannot be measured with the delayed self-heterodyne method as conducted in near-IR wavelengths because of the high dependence on specially ZBLAN fiber.

Overall, the heavily doped soft glass fibers significantly improved the output power and extended the operating wavelengths of single-frequency fiber lasers. However, there are still some limitations with respect to the applications. First, it is the compatibility between the active specialty fiber and the passive silica fiber presented in other fiber components of the laser cavity and in turn the mechanical strength of the splice joints, owing to the different physical properties of these two glasses. Second, although fusion splicing between the highly doped soft glass fiber and silica fiber with low loss can be accomplished with specialized fusion processes, it is still challenging and requires careful handling [82–84]. Furthermore, as for these single-frequency fiber lasers, their dependence on the custom-made heavily doped fibers goes against the broad proliferation into a myriad of applications.

On the other hand, some commercial rare-earth-doped silica fibers can provide high gain coefficients with the development of fiber fabrication techniques, which enables efficient pump absorption [85–87]. Associated with the low-loss of all-silica fiber systems, single-frequency fiber lasers built with these active silica fibers are much more competitive, especially for short-cavity schemes. Efficient single-frequency operation covering three key wavelength bands (the 1, 1.5, and 2 μm region) has been achieved with commercial active silica fibers [88–92]. For example, a single-frequency fiber laser at 1950 nm demonstrated with a standard product from Nufern (PM-TDF-10P/130) [88] shows that 18 mW single-longitudinal-mode output can be obtained with 1.9 cm long Tm^{3+}-doped silica fiber.

3. PERFORMANCE IMPROVEMENTS IN LASER NOISE AND LINEWIDTH OF SINGLE-FREQUENCY FIBER LASERS

A. Noise Suppression of Single-Frequency Fiber Lasers

In addition to high output power, operation with low noise is also required for single-frequency fiber lasers in applications such as interferometric fiber sensing and laser cooling. For fiber lasers, the origins of the intensity and frequency noise are generally given as follows [93–97]: spontaneous emission of the gain medium, fundamental thermal fluctuations inside the resonator, pump efficiency perturbations, and environmental disturbances. To date, many techniques have been developed to suppress the intensity and frequency noise of single-frequency fiber lasers. The common methods for noise reduction are electronic feedback [98–102] and optical feedback [103–106]. Given the advanced status of electronics, electronic feedback was applied in the early stage of the single-frequency fiber laser development. In 1993, Ball introduced a feedback circuit to a single-frequency DBR fiber laser system, and the low-frequency intensity noise, especially at the relaxation oscillation frequency, was efficiently decreased from −82.1 to −112.1 dB/Hz with feedback control [98]. Optoelectronic negative feedback also provides a solution for frequency noise suppression. Cranch presented a technique by phase locking the laser emission to a reference cavity [107], in which the acquired feedback signal is transferred to a compensating strain applied to the laser cavity through a piezoelectric transducer. Thus, the frequency noise spectral density of the single-longitudinal-mode DFB fiber laser is reduced by as much as 20 dB over the frequency range of 1 Hz–10 kHz. However, regardless of intensity noise or frequency noise suppression, the inherent bandwidth limitation of the electronic servo system in the optoelectronic-based feedback approach is inevitable. Additionally, extra electronic noise introduced to the feedback system was observed to weaken the noise suppression [108].

Optical feedback technology has been developed in recent years for linewidth narrowing, noise suppression, and other tasks. In 2012, Zhao *et al.* investigated the effects of self-injection locking on a DFB fiber laser [105], where a stable lasing mode was enhanced with other modes inhibited and the RIN was suppressed by about 16 dB around the relaxation oscillation frequency. Even so, the resulting RIN was still far above the shot noise limit with an average noise level of −120 dB/Hz toward high frequencies due to the noise of the residual pump power still circulating in the feedback loop. Compared to that, a passive optical feedback loop was proved to be more efficient to improve the noise properties of the laser, where the composite cavity can be obtained with the cavity mirrors of the DBR fiber laser and feedback loop [106]. With continuous signal feedback and extended optical path induced longer photon lifetime, both frequency and intensity noise are suppressed remarkably. Furthermore, the semiconductor optical amplifier (SOA) was also introduced to the self-injection locking configuration [108] since the nonlinear amplification dynamics of the SOA can achieve a significant RIN reduction without the broadening of the laser linewidth [109–112].

As shown in Fig. 4, by self-injection locking incorporating an SOA, the frequency noise of the fiber laser was reduced at frequencies higher than 500 Hz, and a maximum reduction was about 25 dB. As for intensity noise, after adding the SOA into the self-injection system, a total reduction of about 35 dB at the relaxation oscillation peak to −125 dB/Hz was achieved. However, as shown in Fig. 4(b), the intensity noise is still well above the shot noise limit, especially at the low frequency. As we stated above, the low-frequency noise caused by the pump noise and external disturbances, can be eliminated with an optoelectronic feedback circuit. Therefore, to achieve the broad-bandwidth near-shot-noise limited-intensity noise suppression, a combination of an SOA and the optoelectronic feedback on its drive current was exploited [113]. Eventually, a maximum noise suppression of 50 dB around the relaxation oscillation frequencies and a suppression bandwidth of up to 50 MHz were achieved. The relative intensity noise in the frequency range from 0.8 kHz to 50 MHz is suppressed to be −150 dB/Hz, which is near the shot noise limit.

B. Linewidth Narrowing of Single-Frequency Fiber Lasers

Single-frequency fiber lasers have marvelous performance in terms of laser linewidth, which results in ultralong coherence length. However, as observed in Table 1, after decades of

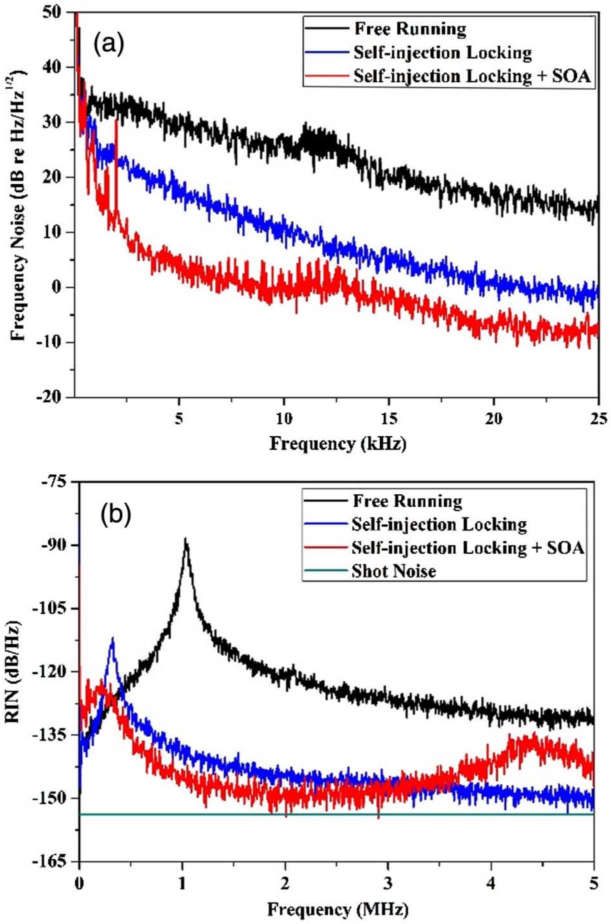

Fig. 4. (a) Measured frequency noise spectra and (b) RINs of the fiber laser at states of free running, self-injection locking, and self-injection locking with SOA.

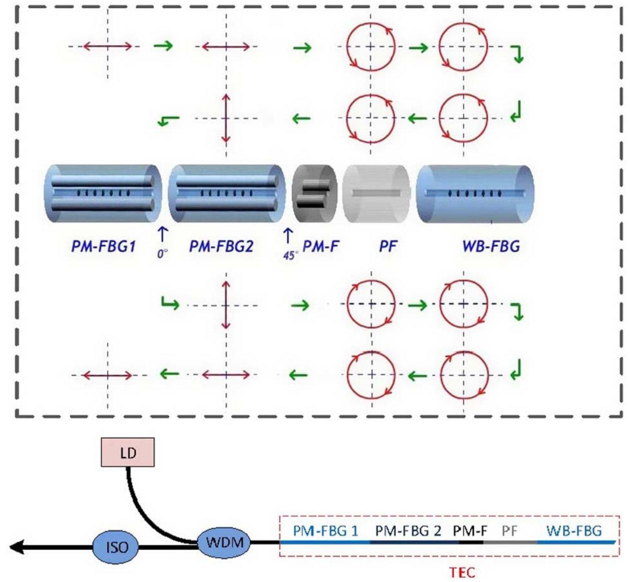

Fig. 5. Experimental setup of the folded-ring-cavity fiber laser. Inset: an exploded view of the cavity structure (not to scale) and an illustration of one possible case of the states of polarization of the light waves travelling inside the cavity (green arrows indicate the directions of the light waves).

development, the linewidth of traditional single-frequency fiber lasers is still limited to several kilohertz, even though efforts, such as temperature control to the laser cavity [53] or integration in an acoustically damped package [46,52], have been devoted to achieving a laser with narrower linewidth. On the other hand, the demand to improve detection range and resolution for applications including high-precision sensing and metrology urges the pursuit of further linewidth compression.

1. Virtual-Folded-Ring Cavity

To further compress the linewidth of a short-linear-cavity fiber laser, a virtual-folded-ring configuration, which combines the advantages of ring lasers and short-linear-cavity lasers, was proposed by Mo *et al.* [114]. As shown in Fig. 5, a piece of polarization-maintaining fiber (PM-F) was used inside the cavity, acting as an all-fiber quarter-wave plate to achieve polarization retardation. By retarding the polarization of the travelling waves, spatial hole burning was diminished and the effective cavity length was extended to nearly twice its physical length. As a result, a single-frequency laser output with a linewidth of less than 820 Hz was obtained from the free-running fiber laser. Afterwards, an FBG-based Fabry–Perot filter [115,116] was inserted between the polarization-maintaining fiber and gain fiber to introduce a slow light effect to the laser cavity, in which multiple reflections extended the photon lifetime of the resonator, allowing more photons to be stored inside the resonator and thus relatively suppressing the contribution of phase diffusion due to spontaneous emission. In this way, the corresponding linewidth of the short-linear-cavity fiber laser was further compressed to <600 Hz. It should be noted that although the folded-ring cavity can effectively eliminate the spatial hole burning and narrow the laser linewidth, manufacturing the laser cavity is not easy. For instance, the PM-F, serving as a quarter-wave plate, should be accurately controlled in length and fused to other parts of the laser cavity with a bias angle of 45°. Furthermore, the temperature disturbance induced by the heat dissipation for both the pump and signal would also affect the function of the PM fiber, which demands extra temperature control.

2. Rayleigh Scattering

Rayleigh scattering as an important component of the scattering in fibers has been observed to possess a scattering bandwidth of tens of kilohertz [117,118], which was utilized to develop a new method of linewidth compression—Rayleigh backscattering (RBS). Since the accumulation of Rayleigh scattering generally needs long optical fiber [119], another effect, stimulated Brillouin scattering (SBS) can build up quickly due to the much higher gain coefficient [120]. For practical applications on the narrow-linewidth fiber laser, some high-RBS fiber structures, such as nonuniform fiber with continuous change of core size and dispersion [121] and long fiber with periodical tapered structure [122], were employed. For instance, Zhu *et al.* presented a ring cavity structure, where the RBS in the tapered optical fiber worked as a linewidth compression element, accompanied by the self-rejection locking technique to further suppress the mode hopping and stabilize output [118]. The narrowest laser linewidth of 130 Hz was achieved with a side-mode suppression ratio up to 75 dB. Moreover, the RBS has been implemented to generate a dual-wavelength fiber laser with a linewidth of 100 Hz. Wavelength-tunable operation was realized without the degradation of laser linewidth [123,124]. The fiber structures with high RBS coefficients suppressed the SBS effect to some extent, whereas the laser power was limited to several milliwatts. On the one hand, the nonuniform fiber with hundred meters in length increased the system loss. More important is that the SBS restriction was still limited, especially under high pump power. For the 5.7 km nonuniform fiber used in [121], the SBS effect occurred just at the signal power of 25 mW. Furthermore, the long fiber system makes it susceptible to the fluctuation of the ambient temperature and noise. Overall, to improve the performance of the RBS-based fiber laser, novel structures with better SBS restriction and short fiber employment should be further considered, such as specially designed photonic crystal fiber [125].

3. Brillouin Fiber Laser

Even though the SBS is an obstacle for the development of high-power fiber lasers and amplifiers [126,127], it provides an effective technical solution on linewidth narrowing of fiber lasers. Based on the three-wave model of SBS, a study implemented in [128,129] showed that phase noise of the pump laser is transferred to the emitted Stokes wave after being strongly reduced and smoothed under the combined influence of acoustic damping and cavity feedback. The resulting Stokes linewidth can be several orders of magnitude narrower than that of the pump laser [130,131]. However, due to the limited Brillouin gain coefficient, a critically pump-coupled fiber resonator [132] or high pump threshold power [133,134] is generally needed for a Brillouin fiber laser. Afterwards, a rare-earth-doped fiber amplifier was introduced to the Brillouin ring cavity to provide the gain for both the pump laser and the generated Stokes light [135,136]. The proposed scheme compensates the resonator losses and simplifies the laser system. A typical example is the Brillouin/erbium fiber laser (BEFL), which has been investigated thoroughly in linewidth narrowing of the fiber laser [137–139]. The analysis on the linewidth narrowing effect in BEFL launched by Chen *et al.* showed that the linear gain of active fiber played an important role in the strong linewidth reduction of BEFL [131]. The resulting demonstration of BEFL transferred a 20 MHz Brillouin pump into 950 Hz Brillouin Stokes laser emission, which obtained over four orders of magnitude of linewidth reduction. In 2015, an ultranarrow linewidth of 40 Hz was presented in a BEFL scheme with only 45 cm erbium-doped fiber [140]. Compared with the Brillouin pump with a linewidth of 20 MHz, the achieved 40 Hz laser linewidth from BEFL measured with the heterodyne beat technique is reduced by five orders of magnitude. The theoretical analysis [131,140] indicated that the strong linewidth reduction was due to the low cavity loss rate in assistance of the linear gain of the erbium-doped fiber and large light amplitude feedback.

To ensure a clear format, the noise suppression and linewidth narrowing for the single-frequency fiber laser were respectively reviewed here. However, these two aspects are not independent, especially for the phase noise to the laser linewidth since the frequency fluctuations of the laser cause a broadening of its line shape. The relation between laser linewidth and frequency noise spectral density has been addressed in [97], and the information about the laser linewidth can be extracted from the frequency noise spectra in geometric approaches. This relationship was also indicated in our reviewed papers: when the frequency noise of the single-frequency fiber laser system was well suppressed, the laser linewidth would be narrowed correspondingly and vice versa. For example, as introduced in Section 3.A, the all-optical noise suppression was achieved by virtue of self-injection locking incorporated with SOA. From Fig. 4(a), about 15 dB of frequency noise reduction can be observed at frequencies higher than 500 Hz with the self-injection locking and further reduction of 10 dB was realized when incorporating SOA into the system. As for the measured laser linewidth, the 3.5 kHz Lorentz linewidth of the free-running fiber laser was decreased to 1.1 kHz when self-injection locked and to 700 Hz when self-injection locked with SOA. Therefore, to improve the performance of a single-frequency fiber laser, comprehensive consideration should be given to all the parameters, including output power, laser linewidth, intensity, and frequency noise.

Furthermore, one should learn that the linewidth of a single-frequency fiber laser is generally measured with the method of delayed self-heterodyne or heterodyne, using a narrower-linewidth laser as the reference signal. The beat note was then analyzed with a RF spectrum analyzer, and the measurement time is usually on the millisecond level [141,142]. Accordingly, the laser linewidth that we mentioned here can be approximately taken as the instantaneous linewidth [143,144]. As we know, the laser line shape can be fitted with a Voigt profile, which is a convolution of a Lorentzian and a Gaussian function. The Lorentzian part corresponds to the white noise arising from the spontaneous emission, which is viewed as the intrinsic linewidth of the laser. The Gaussian part of the Voigt function corresponds to the 1/f noise, which arises from of the pump fluctuation and "technical noise," such as the environment disturbances. When it comes to the relative linewidth over time, it can be expected that [145] the Lorentzian linewidth, which is not sensitive to low-frequency noise, would not change much. In contrast, the Gaussian part would increase as the increasing 1/f noise contributes to the laser linewidth at longer observation time. This makes it necessary that a well-handled temperature control system for the whole laser cavity and an isolated enclosure to protect from the environmental disturbances are included to the laser system.

4. PROGRESS OF SINGLE-FREQUENCY FIBER AMPLIFIERS

A. High-Power CW Single-Frequency Fiber Amplifiers

For higher laser power achievement, single-frequency fiber sources are generally configured as a high-gain fiber master oscillation power amplifier (MOPA), which is seeded by a low-power, single-frequency oscillator and then followed by a series of amplifier stages to realize power amplification, as

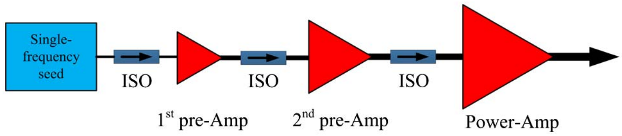

Fig. 6. Schematic of a typical single-frequency fiber MOPA with three amplifier stages.

shown in Fig. 6. The configuration provides an excellent means for power scaling while preserving the characteristics of a single-frequency seed as much as possible. For such a device, all-fiber structure is preferable to simplify the configurations with improved compactness and reliability since the free-space components need careful beam alignment, resulting in high ASE noise and a degraded polarization-extinction ratio in a linear polarized system. Although the laser power for the single-mode fiber laser has reached the 10 kW level [8], the all-fiber single-frequency amplifiers just obtain an output power of several hundreds of watts up to now, which is restricted by severe nonlinear effect due to the narrow linewidth, particularly the SBS [63,126,146].

The output power evolution of CW single-frequency amplifiers with all-fiber format operation in the regimes of 1, 1.5, and 2 μm is summarized and shown in Fig. 7. Even for the most powerful gain fiber material—Yb^{3+}-doped fiber—the maximum output power reported so far is around 414 W at 1064 nm for an all-fiber laser under single-frequency operation [147–150]. A short, highly Yb^{3+}-doped LMA was utilized in the power amplifier stage to suppress the nonlinearity, including SBS. Step-distributed longitudinal strain is imposed on the active fiber to broaden its effective SBS gain spectrum and further increase the SBS threshold. Furthermore, proper thermal management of the active fiber under such high gain is required for steady laser operation, so water cooling should be employed to the highly Yb^{3+}-doped LMA fiber. To alleviate the SBS effect, other different approaches [151–156], such as co-amplified with a broad signal [151], acoustically tailored active PCF [152] and core in-band pump [153], have been proposed successively for high-power single-frequency amplification. With the acoustic- and gain-tailored Yb^{3+}-doped PCF, C. Robin *et al.* achieved a record single-frequency output power of 811 W with near diffraction-limited beam quality [152]. Distinct transverse acoustic regions were created in the core of the Yb^{3+}-doped PCF to introduce multiple transverse Brillouin frequencies, which suppressed the SBS effectively in conjunction with externally applied thermal gradient. Moreover, with the development of heavily rare-earth-doped LMA soft glass fiber, extractable power within the SBS threshold has been theoretically analyzed [60,157], which implies a promising path to obtain high power in a compact fiber system.

In the 1.5 μm region, the Er^{3+}/Yb^{3+}-codoped fiber was proposed to provide a solution to the concentration quenching in pure Er^{3+}-doped fiber, and the increased pump absorption at 976 nm makes the power scaling at 1.5 μm available. Nevertheless, the Er^{3+}/Yb^{3+}-codoped fiber amplifiers typically suffer from severe Yb^{3+}-ASE or even parasitic lasing at 1 μm and consequently result in an efficiency reduction for the 1.5 μm laser [126,158]. This hinders the demonstration of high power amplification in this regime [159–162], which can be found from Fig. 7. Recently, Creeden *et al.* demonstrated single-frequency amplification to 207 W average output power in an Er^{3+}/Yb^{3+}-codoped LMA fiber [163]. An optical efficiency of 49.3% (slope efficiency of 50.5%) was achieved in their demonstration, which is the highest reported efficiency from a high-power 9×× nm pumped Er^{3+}/Yb^{3+}-doped fiber amplifier. The amplification adopted a pump wavelength of 940 nm instead of 976 nm. By pumping off-peak at 940 nm, the Yb^{3+} inversion versus length is accordingly decreased and thus suppresses the 1 μm ASE/lasing at the high-pump-power level. The bottlenecking problem of the energy transfer from Yb^{3+} to Er^{3+} was partially solved with the efficiency improvement in the 1.5 μm region.

The cross-relaxation process of Tm^{3+} due to the specific energy-level structure enables its quantum efficiency close to two [126]. Combined with double-cladding pump technology, the power scaling of 2 μm fiber lasers has developed rapidly over the last 10 years. With the intense research interest in this regime, laser power of the single-frequency amplification has been significantly improved [164–169]. In 2009, Goodno *et al.* demonstrated a single-frequency Tm-doped fiber amplifier with an output power of 608 W at 2040 nm. This is up to now the highest output power for single-frequency fiber amplifier around 2 μm, even though with a free-space pump coupling in the power amplifier stage. The laser power was only limited by the available pump power rather than the SBS effect. It is estimated that the SBS-free single frequency will be limited to ∼750 W by the passive exit pigtail, where the SBS can be accumulated dramatically. For the all-fiber MOPA configuration, an output power of 100 W was not realized until 2013 with the development of high-power fiber devices in 2 μm [166]. Afterwards, the output power was rapidly increased to 310 W accompanying proper parameters of the gain fibers and reasonable arrangement of the MOPA system [169]. Furthermore, the heavily Tm^{3+}-doped germanate glass fiber was examined to be an efficient gain medium for power scaling. In 2016, Yang *et al.* amplified a 350 mW single-frequency laser at 1.95 μm to 11.7 W with only 31 cm of long, heavily Tm^{3+}-doped germanate fiber [170]. Such a high gain provided by the

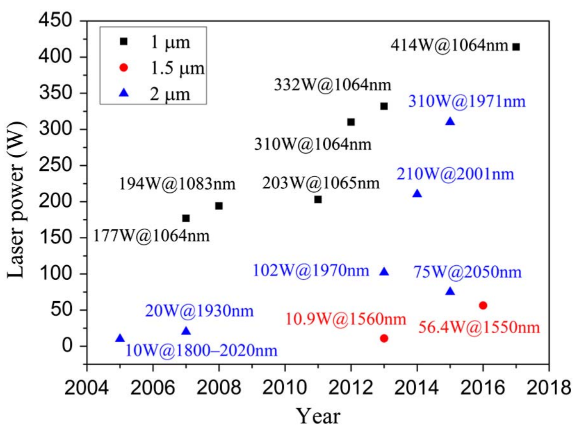

Fig. 7. Output power evolution of CW single-frequency amplifiers in all-fiber format operating in 1, 1.5, and 2 μm regions.

short active fiber would significantly increase the threshold of SBS, providing a competitive candidate for the generation of a 2 μm high-power single-frequency fiber amplifier.

Raman fiber devices [171], in which stimulated Raman scattering (SRS) provides gain, can be used to generate high-power lasers in the spectral regime where rare-earth-doped fiber lasers cannot cover. A typical single-frequency Raman fiber amplifier is generally backward pumped to maintain narrow linewidth, and the pump wavelength is determined by the Raman shift of the silica fiber. SBS is the main limiting factor in power scaling of single-frequency Raman fiber amplifiers due to the two orders of magnitude higher gain coefficient [119]. To improve the amplifier efficiency, SBS has to be suppressed effectively. Acoustically tailored optical fibers through the manipulation of the concentration of dopants in the core were explored to reduce the Brillouin gain, while maintaining or even enhancing Raman gain [172,173]. Up to 22 W single-frequency 1178 nm output was reported in a backward-pumped two-stage amplifier with an optical efficiency of about 25% [168]. By applying thermal gradients along the gain fiber, 1.5 times improvement of the SBS threshold was achieved in a single-stage amplifier experiment [174].

Applying longitudinally varied strain according to the power distribution along the gain fiber was also discussed to suppress SBS in single-frequency Raman fiber amplifiers [175]. As shown in Fig. 8, 30 strain steps were employed in a 50 m long gain fiber and the fiber length for different strain steps varies significantly. This is very different from the suppression of SBS in passive delivery fiber, where uniform strain steps are close to the optimum. With this method, the highest output of 84 W was demonstrated for single-frequency Raman fiber amplifiers [176].

For a Raman fiber device, the advantage in wavelength versatility facilitates its operation at any wavelength where the optical gain fiber is transparent, only if an appropriate pump laser was provided. Therefore, the developed technology of a single-frequency Raman fiber amplifier can be applied to many other applications which require high-power laser at a specific wavelength not convenient for rare-earth-doped fiber lasers.

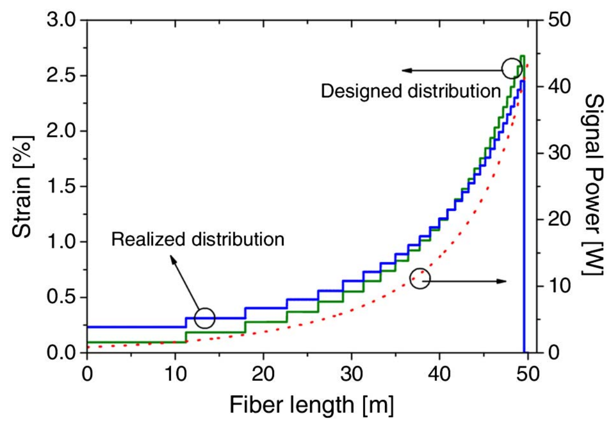

Fig. 8. Calculated signal power evolution (dotted, red), the designed strain distribution (solid, green), and the applied strain distribution (solid, blue) along the fiber.

B. High-Power/Energy Pulsed Single-Frequency Fiber Amplifiers

Some practical applications, such as coherent LIDAR, remote sensing, and nonlinear frequency conversion, require single-frequency fiber-laser pulsed operation with high energy or peak power. However, neither directly *Q*-switching a DBR single-frequency fiber laser nor modulating a CW single-frequency fiber laser with an intensity modulator can provide enough energy or power for practical applications [126]. A high-gain MOPA laser system is usually needed to further scale up the power/energy of the single-frequency pulses. As we discussed above, the power scaling of the narrow-linewidth fiber laser is primarily restricted by the SBS effect due to the limited core diameter. Therefore, different strategies, which have been employed to enhance the SBS threshold in single-frequency pulsed MOPA systems, are summarized here, accompanied by the progress of single-frequency pulsed MOPA demonstrations.

(1) Since the threshold of SBS depends strongly on the fiber core size and fiber length [127], one method is to focus on the optical fiber itself. LMA active fiber [177,178] and short heavily rare-earth-doped soft glass fiber [179–183] have been employed to achieve high-power/energy single-frequency pulsed fiber lasers. In 2010, a kilowatt-level SBS-threshold monolithic single-frequency pulsed fiber laser was demonstrated (shown in Fig. 9) by using short, highly Er^{3+}/Yb^{3+}-codoped phosphate fibers in power amplifier stages [180]. With 15 cm long high-gain phosphate fiber, a peak power of ∼1.2 kW for 105 ns pulses was generated at 1530 nm. Additionally, the highly doped gain fiber also facilitates the achievement of millijoule-level pulse energy in 2 μm with the all-fiber single-frequency nanosecond pulsed laser source [183]. In the final power amplifier of the MOPA configuration, only a piece of 41 cm long large-core (30 μm) highly Tm^{3+}-doped germanate glass fiber was used to efficiently boost the pulse power and energy.

(2)The second is to introduce frequency shift to the SBS gain spectrum along the fiber with a temperature gradient [184] or a strain gradient [185–187]. Thus, the SBS light could not get amplified efficiently in the gain fiber. For the all-fiber work on single-frequency pulsed amplification at 1540 nm demonstrated in 2014 [188], longitudinally varied strains were applied on a 0.8 m long Er^{3+}/Yb^{3+}-codoped PM fiber with a core diameter of 10 μm in the power amplifier stage. The threshold of SBS has been enhanced ∼3.4 times. Peak power of 361 W for 200 ns pulses at a 10 kHz repetition rate was achieved with transform-limited linewidth and diffraction-limited beam quality.

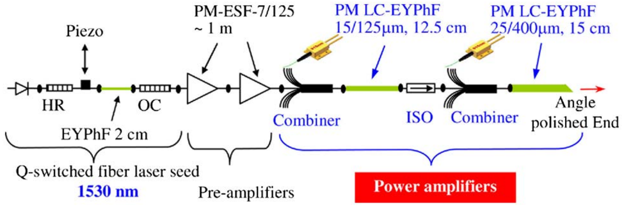

Fig. 9. Schematic of the kilowatt-level SBS-threshold narrow-linewidth pulsed monolithic fiber laser at 1530 nm.

(3) Considering that the SBS is an interaction between photons and phonons in the fiber, the last one is to shorten the pulse duration. If the applications allow, a pulse duration shorter than the phonon lifetime, which is around 10 ns in silica fiber [189], can be adopted to increase the SBS threshold [190–192]. In 2014, an average output power of 913 W for 3 ns pulses at a repetition rate of 10 MHz was achieved in a high-power narrow-linewidth nanosecond fiber amplifier at 1064 nm [193]. The absence of a nonlinear increase of backward power in the main amplifier indicated that SBS was effectively suppressed for short pulse durations. The maximum laser power is not limited by the SBS effect but the SRS, which has a much shorter phonon lifetime of <100 fs.

Furthermore, a combination of different SBS-suppression approaches was also employed to improve the performance of single-frequency pulsed fiber amplifiers [194]. In 2012, over 100 kW peak power, single-frequency pulses were demonstrated by Shi *et al.*, using multiple-stage, short, large-core Er^{3+}/Yb^{3+}-codoped phosphate fibers, in which a short pulse width at a few nanoseconds was employed to further increase the SBS threshold [195]. The same strategy was also applied in the 2 μm regime to demonstrate a kilowatt-peak-power, single-frequency pulsed fiber laser with heavily Tm^{3+}-doped silicate fiber [196].

5. SUMMARY

Single-frequency fiber lasers were briefly reviewed with recent progress in this paper, including recent progress. With the development of heavily rare-earth-doped soft glass fiber, watt-level output power has been achieved for single-frequency fiber oscillators. Performance improvement on laser linewidth and noise has been continuously pushed forward with the newly developed physical mechanisms. Efforts to increase the output power/energy of single-frequency fiber amplifiers have been made with different strategies on the suppression of the SBS effect and even mode instability. One should expect substantial progress in this area with new fiber designs and system architectures. All of this would further motivate the applications of single-frequency fiber lasers in broader areas from science, defense, and industry to our daily life.

Funding. National Natural Science Foundation of China (NSFC) (61275102, 61335013); National High Technology Research and Development Program (2014AA041901); National Basic Research Program of China (2014CB3399802); Regional Demonstration Projects of Ocean Economic Innovation Development (cxsf2014-21); Doctoral Fund of Ministry of Education (20130032110051).

REFERENCES

1. C. J. Koester and E. Snitzer, “Amplification in a fiber laser,” Appl. Opt. **3**, 1182–1186 (1964).
2. A. Tünnermann, T. Schreiber, and J. Limpert, “Fiber lasers and amplifiers: an ultrafast performance evolution,” Appl. Opt. **49**, F71–F78 (2010).
3. D. S. Funk, J. W. Carlson, and J. G. Eden, “Ultraviolet (381 nm), room temperature laser in neodymium-doped fluorozirconate fibre,” Electron. Lett. **30**, 1859–1860 (1994).
4. T. P. Baraniecki, R. Caspary, and W. Kowalsky, “Blue, green, red fiber lasers based on Pr/Yb fluoride fibers,” in *6th International Conference on Transparent Optical Networks* (IEEE, 2004), Vol. **2**.
5. J. Nilsson, W. A. Clarkson, R. Selvas, J. K. Sahu, P. W. Turner, S. U. Alam, and A. B. Grudinin, “High-power wavelength-tunable cladding-pumped rare-earth-doped silica fiber lasers,” Opt. Fiber Technol. **10**, 5–30 (2004).
6. R. Vallee, V. Fortin, M. Bernier, S. Duval, F. Maes, and F. Jobin, “Recent development in mid-infrared fluoride glass fiber lasers,” in *Photonics and Fiber Technology (ACOFT, BGPP, NP)*, OSA Technical Digest (Optical Society of America, 2016), paper AM2C.1.
7. S. D. Jackson, “Mid-IR fiber lasers,” in *Advanced Photonics (IPR, NOMA, Sensors, Networks, SPPCom, SOF)*, OSA Technical Digest (Optical Society of America, 2016), paper SoTu3G.3.
8. M. O’Connor, V. Gapontsev, V. Fomin, M. Abramov, and A. Ferin, “Power scaling of SM fiber lasers toward 10 kW,” in *Conference on Lasers and Electro-Optics/International Quantum Electronics Conference*, OSA Technical Digest (Optical Society of America, 2009), paper CThA3.
9. F. Stutzki, F. Jansen, A. Liem, C. Jauregui, J. Limpert, and A. Tünnermann, “26 mJ, 130 W *Q*-switched fiber-laser system with near-diffraction-limited beam quality,” Opt. Lett. **37**, 1073–1075 (2012).
10. G. Krauss, S. Lohss, T. Hanke, A. Sell, S. Eggert, R. Huber, and A. Leitenstorfer, “Synthesis of a single cycle of light with compact erbium-doped fiber technology,” Nat. Photonics **4**, 33–36 (2010).
11. A. Sell, G. Krauss, R. Scheu, R. Huber, and A. Leitenstorfer, “8-fs pulses from a compact Er:fiber system: quantitative modeling and experimental implementation,” Opt. Express **17**, 1070–1077 (2009).
12. S. S. Sané, S. Bennetts, J. E. Debs, C. C. N. Kuhn, G. D. McDonald, P. A. Altin, J. D. Close, and N. P. Robins, “11 W narrow linewidth laser source at 780 nm for laser cooling and manipulation of rubidium,” Opt. Express **20**, 8915–8919 (2012).
13. V. Kuhn, D. Kracht, J. Neumann, and P. Weßels, “Er-doped single-frequency photonic crystal fiber amplifier with 70 W of output power for gravitational wave detection,” Proc. SPIE **8237**, 82371G (2012).
14. T. Wu, X. Peng, W. Gong, Y. Zhan, Z. Lin, B. Luo, and H. Guo, “Observation and optimization of 4 He atomic polarization spectroscopy,” Opt. Lett. **38**, 986–988 (2013).
15. G. Canat, B. Augère, C. Besson, A. Dolfi-Bouteyre, A. Durecu, D. Goular, J. L. Gouët, L. Lombard, C. Planchat, and M. Valla, “High peak power single-frequency MOPFA for lidar applications,” in *Conference on Lasers and Electro-Optics*, OSA Technical Digest (Optical Society of America, 2016), paper AM3K.4.
16. A. Chavez-Pirson, “Highly doped phosphate glass fibers for fiber lasers and amplifiers with applications,” Proc. SPIE **7839**, 78390K (2010).
17. Y. Jeong, J. Nilsson, J. K. Sahu, D. N. Horley, L. M. B. Hickey, and P. W. Turner, “Power scaling of single-frequency ytterbium-doped fiber master-oscillator power-amplifier sources up to 500 W,” IEEE J. Sel. Top. Quantum Electron. **13**, 546–551 (2007).
18. M. Ibsen, Z. Zhang, L. Pearson, J. W. Kim, J. K. Sahu, and W. A. Clarkson, “High power single-frequency fibre lasers: design and applications,” in *15th Optoelectronics and Communications Conference* (OECC, 2010), pp. 182–183.
19. I. M. Jauncey, L. Reekie, J. E. Townsend, D. N. Payne, and C. J. Rowe, “Single-longitudinal-mode operation of an Nd^{3+}-doped fibre laser,” Electron. Lett. **24**, 24–26 (1988).
20. L. Dong, W. H. Loh, J. E. Caplen, J. D. Minelly, K. Hsu, and L. Reekie, “Efficient single-frequency fiber lasers with novel photosensitive Er/Yb optical fibers,” Opt. Lett. **22**, 694–696 (1997).
21. J. Shi, S. Alam, and M. Ibsen, “Sub-watt threshold, kilohertz-linewidth Raman distributed-feedback fiber laser,” Opt. Lett. **37**, 1544–1546 (2012).
22. G. A. Ball, W. W. Morey, and W. H. Glenn, “Standing-wave monomode erbium fiber laser,” IEEE Photon. Technol. Lett. **3**, 613–615 (1991).
23. C. P. Spiegelberg, “Compact 100 mW fiber laser with 2 kHz linewidth,” in *Optical Fiber Communication Conference*, OSA Technical Digest (Optical Society of America, 2003), paper PD45.

24. T. Qiu, S. Suzuki, A. Schülzgen, L. Li, A. Polynkin, V. Temyanko, J. V. Moloney, and N. Peyghambarian, "Generation of watt-level single-longitudinal-mode output from cladding-pumped short fiber lasers," Opt. Lett. **30**, 2748–2750 (2005).
25. S. Srivastava, R. Gopal, S. Sai, and K. Srinivasan, "Feedback Mach–Zehnder resonator with reflector: analysis and applications in single frequency fiber lasers," Appl. Phys. Lett. **89**, 141118 (2006).
26. Z. Meng, G. Stewart, and G. Whitenett, "Stable single-mode operation of a narrow-linewidth, linearly polarized, erbium-fiber ring laser using a saturable absorber," J. Lightwave Technol. **24**, 2179–2183 (2006).
27. S. Feng, Q. Mao, Y. Tian, Y. Ma, W. Li, and L. Wei, "Widely tunable single longitudinal mode fiber laser with cascaded fiber-ring secondary cavity," IEEE Photon. Technol. Lett. **25**, 323–326 (2013).
28. W. H. Loh, B. N. Samson, L. Dong, G. J. Cowle, and K. Hsu, "High performance single frequency fiber grating-based erbium: ytterbium-codoped fiber lasers," J. Lightwave Technol. **16**, 114–118 (1998).
29. Y. O. Barmenkov, D. Zalvidea, S. Torres-Peiró, J. L. Cruz, and M. V. Andrés, "Effective length of short Fabry–Perot cavity formed by uniform fiber Bragg gratings," Opt. Express **14**, 6394–6399 (2006).
30. A. Polynkin, P. Polynkin, M. Mansuripur, and N. Peyghambarian, "Single-frequency fiber ring laser with 1 W output power at 1.5 μm," Opt. Express **13**, 3179–3184 (2005).
31. F. D. Muhammad, M. Z. Zulkifli, A. A. Latif, S. W. Harun, and H. Ahmad, "Graphene-based saturable absorber for single-longitudinal-mode operation of highly doped erbium-doped fiber laser," IEEE Photon. J. **4**, 467–475 (2012).
32. T. Wang, T. Yang, D. Jia, Z. Wang, and C. Ge, "Multi-wavelength lasers with suppressed spectral linewidth of 10 kHz," Opt. Express **22**, 26862–26871 (2014).
33. S. Jiang, B. Hwang, T. Luo, K. Seneschal, N. Peyghambarian, F. Smektala, S. Honkanen, and J. Lucas, "Net gain of 15.5 dB from a 5.1 cm-long Er^{3+}-doped phosphate glass fiber," in *Optical Fiber Communication Conference*, OSA Technical Digest Series (Optical Society of America, 2000), paper PD5.
34. S. Jiang, "Thulium-doped heavy metal oxide glasses for 2 μm lasers," U.S. patent 7,298,768 (November 20, 2007).
35. X. Zhu, W. Shi, J. Zong, D. Nguyen, R. A. Norwood, A. Chavez-Pirson, and N. Peyghambarian, "976 nm single-frequency distributed Bragg reflector fiber laser," Opt. Lett. **37**, 4167–4169 (2012).
36. M. J. Digonnet, *Rare-Earth-Doped Fiber Lasers and Amplifiers, Revised, and Expanded* (CRC Press, 2001).
37. T. Ohtsuki, N. Peyghambarian, S. Honkanen, and S. I. Najafi, "Gain characteristics of a high concentration Er^{3+}-doped phosphate glass waveguide," J. Appl. Phys. **78**, 3617–3621 (1995).
38. D. Creeden, B. R. Johnson, G. A. Rines, and S. D. Setzler, "High power resonant pumping of Tm-doped fiber amplifiers in core- and cladding-pumped configurations," Opt. Express **22**, 29067–29080 (2014).
39. G. Tang, T. Zhu, W. Liu, W. Lin, T. Qiao, M. Sun, D. Chen, Q. Qian, and Z. Yang, "Tm^{3+} doped lead silicate glass single mode fibers for 2.0 μm laser applications," Opt. Mater. Express **6**, 2147–2157 (2016).
40. X. Wen, G. Tang, Q. Yang, X. Chen, Q. Qian, Q. Zhang, and Z. Yang, "Highly Tm^{3+}-doped germanate glass and its single mode fiber for 2.0 μm laser," Sci. Rep. **6**, 20344 (2016).
41. Y. C. Yan, A. J. Faber, H. de Waal, P. G. Kik, and A. Polman, "Erbium-doped phosphate glass waveguide on silicon with 4.1 dB/cm gain at 1.535 μm," Appl. Phys. Lett. **71**, 2922–2924 (1997).
42. J. Wu, S. Jiang, T. Luo, J. Geng, N. Peyghambarian, and N. P. Barnes, "Efficient thulium-doped 2-μm germanate fiber laser," IEEE Photon. Technol. Lett. **18**, 334–336 (2006).
43. T. Qiu, L. Li, A. Schulzgen, V. L. Temyanko, T. Luo, S. Jiang, A. Mafi, J. V. Moloney, and N. Peyghambarian, "Generation of 9.3-W multimode and 4-W single-mode output from 7-cm short fiber lasers," IEEE Photon. Technol. Lett **16**, 2592–2594 (2004).
44. Y. Hu, S. Jiang, T. Luo, K. Seneschal, M. Morrell, F. Smektala, S. Honkanen, J. Lucas, and N. Peyghambarian, "Performance of high-concentration Er^{3+}-Yb^{3+}-codoped phosphate fiber amplifiers," IEEE Photon. Technol. Lett. **13**, 657–659 (2001).
45. Y. Kaneda, C. Spiegelberg, J. Geng, Y. Hu, T. Luo, and S. Jiang, "200-mW, narrow-linewidth 1064.2-nm Yb-doped fiber laser," in *Conference on Lasers and Electro-Optics/International Quantum Electronics Conference and Photonic Applications Systems Technologies*, OSA Technical Digest (Optical Society of America, 2004), paper CThO3.
46. S. Xu, Z. Yang, W. Zhang, X. Wei, Q. Qian, D. Chen, Q. Zhang, S. Shen, M. Peng, and J. Qiu, "400 mW ultrashort cavity low-noise single-frequency Yb^{3+}-doped phosphate fiber laser," Opt. Lett. **36**, 3708–3710 (2011).
47. S. Xu, C. Li, W. Zhang, S. Mo, C. Yang, X. Wei, Z. Feng, Q. Qian, S. Shen, M. Peng, Q. Zhang, and Z. Yang, "Low noise single-frequency single-polarization ytterbium-doped phosphate fiber laser at 1083 nm," Opt. Lett. **38**, 501–503 (2013).
48. C. Yang, Q. Zhao, Z. Feng, M. Peng, Z. Yang, and S. Xu, "1120 nm kHz-linewidth single-polarization single-frequency Yb-doped phosphate fiber laser," Opt. Express **24**, 29794–29799 (2016).
49. C. Spiegelberg, J. Geng, Y. Hu, Y. Kaneda, S. Jiang, and N. Peyghambarian, "Low-noise narrow-linewidth fiber laser at 1550 nm (June 2003)," J. Lightwave Technol. **22**, 57–62 (2004).
50. P. Polynkin, A. Polynkin, M. Mansuripur, J. Moloney, and N. Peyghambarian, "Single-frequency laser oscillator with watts-level output power at 1.5 μm by use of a twisted-mode technique," Opt. Lett. **30**, 2745–2747 (2005).
51. A. Schülzgen, L. Li, V. L. Temyanko, S. Suzuki, J. V. Moloney, and N. Peyghambarian, "Single-frequency fiber oscillator with watt-level output power using photonic crystal phosphate glass fiber," Opt. Express **14**, 7087–7092 (2006).
52. S. H. Xu, Z. M. Yang, T. Liu, W. N. Zhang, Z. M. Feng, Q. Y. Zhang, and Z. H. Jiang, "An efficient compact 300 mW narrow-linewidth single frequency fiber laser at 1.5 μm," Opt. Express **18**, 1249–1254 (2010).
53. P. Hofmann, C. Voigtländer, S. Nolte, N. Peyghambarian, and A. Schülzgen, "550-mW output power from a narrow linewidth all-phosphate fiber laser," J. Lightwave Technol. **31**, 756–760 (2013).
54. J. Geng, J. Wu, S. Jiang, and J. Yu, "Efficient operation of diode-pumped single-frequency thulium-doped fiber lasers near 2 μm," Opt. Lett. **32**, 355–357 (2007).
55. J. Geng, Q. Wang, T. Luo, S. Jiang, and F. Amzajerdian, "Single-frequency narrow-linewidth Tm-doped fiber laser using silicate glass fiber," Opt. Lett. **34**, 3493–3495 (2009).
56. Q. Yang, S. Xu, C. Li, C. Yang, Z. Feng, Y. Xiao, X. Huang, and Z. Yang, "A single-frequency linearly polarized fiber laser using a newly developed heavily Tm^{3+}-doped germanate glass fiber at 1.95 μm," Chin. Phys. Lett. **32**, 094206 (2015).
57. J. Wu, Z. Yao, J. Zong, A. Chavez-Pirson, N. Peyghambarian, and J. Yu, "Single frequency fiber laser at 2.05 μm based on Ho-doped germanate glass fiber," Proc. SPIE **7195**, 71951K (2009).
58. Y. W. Lee, S. Sinha, M. J. F. Digonnet, R. L. Byer, and S. Jiang, "20 W single-mode Yb^{3+}-doped phosphate fiber laser," Opt. Lett. **31**, 3255–3257 (2006).
59. Y. W. Lee, S. Sinha, M. J. F. Digonnet, R. L. Byer, and S. Jiang, "Measurement of high photo darkening resistance in heavily Yb^{3+}-doped phosphate fibers," Electron. Lett. **44**, 14–16 (2008).
60. Y. W. Lee, M. J. F. Digonnet, S. Sinha, K. E. Urbanek, R. L. Byer, and S. Jiang, "High-power Yb^{3+}-doped phosphate fiber amplifier," IEEE J. Sel. Top. Quantum Electron. **15**, 93–102 (2009).
61. D. C. Hanna, R. M. Percival, I. R. Perry, R. G. Smart, P. J. M. Suni, J. E. Townsend, and A. C. Tropper, "Continuous-wave oscillation of a monomode ytterbium-doped fibre laser," Electron. Lett. **24**, 1111–1113 (1988).
62. H. M. Pask, R. J. Carman, D. C. Hana, A. C. Tropper, C. J. Mackechnie, P. R. Barber, and J. M. Dawes, "Ytterbium-doped silica fiber lasers: versatile sources for the 1–1.2 μm region," IEEE J. Sel. Top. Quantum Electron. **1**, 2–13 (1995).
63. D. J. Richardson, J. Nilsson, and W. A. Clarkson, "High power fiber lasers: current status and future perspectives [Invited]," J. Opt. Soc. Am. B **27**, B63–B92 (2010).
64. P. F. Moulton, G. A. Rines, E. V. Slobodtchikov, K. F. Wall, G. Frith, B. Samson, and A. L. G. Carter, "Tm-doped fiber lasers: fundamentals and power scaling," IEEE J. Sel. Top. Quantum Electron. **15**, 85–92 (2009).

65. Z. Zhang, D. Y. Shen, A. J. Boyland, J. K. Sahu, W. A. Clarkson, and M. Ibsen, "High-power Tm-doped fiber distributed-feedback laser at 1943 nm," Opt. Lett. **33**, 2059–2061 (2008).
66. S. Jiang, "Recent progress on 2-micron fiber lasers," in *Optical Fiber Communication Conference/National Fiber Optic Engineers Conference 2011*, OSA Technical Digest (Optical Society of America, 2011), paper OMQ4.
67. J. Geng, Q. Wang, J. Smith, T. Luo, F. Amzajerdian, and S. Jiang, "All-fiber *Q*-switched single-frequency Tm-doped laser near 2 μm," Opt. Lett. **34**, 3713–3715 (2009).
68. X. He, S. Xu, C. Li, C. Yang, Q. Yang, S. Mo, D. Chen, and Z. Yang, "1.95 μm kHz-linewidth single-frequency fiber laser using self-developed heavily Tm^{3+}-doped germanate glass fiber," Opt. Express **21**, 20800–20805 (2013).
69. J. Geng, Q. Wang, Y. N. Lee, and S. Jiang, "Development of eye-safe fiber lasers near 2 μm," IEEE J. Sel. Top. Quantum Electron. **20**, 150–160 (2014).
70. J. Geng, Q. Wang, T. Luo, B. Case, S. Jiang, F. Amzajerdian, and J. Yu, "Single-frequency gain-switched Ho-doped fiber laser," Opt. Lett. **37**, 3795–3797 (2012).
71. X. Wen, G. Tang, J. Wang, X. Chen, Q. Qian, and Z. Yang, "Tm^{3+} doped barium gallo-germanate glass single-mode fibers for 2.0 μm laser," Opt. Express **23**, 7722–7731 (2015).
72. S. D. Jackson, "Single-transverse-mode 2.5-W holmium-doped fluoride fiber laser operating at 2.86 μm," Opt. Lett. **29**, 334–336 (2004).
73. S. Tokita, M. Murakami, S. Shimizu, M. Hashida, and S. Sakabe, "Liquid-cooled 24 W mid-infrared Er:ZBLAN fiber laser," Opt. Lett. **34**, 3062–3064 (2009).
74. L. B. Shaw, B. Cole, P. A. Thielen, J. S. Sanghera, and I. D. Aggarwal, "Mid-wave IR and long-wave IR laser potential of rare-earth doped chalcogenide glass fiber," IEEE J. Quantum Electron. **37**, 1127–1137 (2001).
75. R. S. Quimby, L. B. Shaw, and I. D. Aggarwal, "Modeling of cascade lasing in Dy:chalcogenide glass fiber laser with efficient output at 4.5 μm," IEEE Photon. Technol. Lett. **20**, 123–125 (2008).
76. X. Zhu and N. Peyghambarian, "High-power ZBLAN glass fiber lasers: review and prospect," Adv. Optoelectron. **2010**, 1–23 (2010).
77. J. Schneider, "Fluoride fibre laser operating at 3.9 μm," Electron. Lett. **31**, 1250–1251 (1995).
78. X. Zhu, J. Zong, R. A. Norwood, A. Chavez-Pirson, and N. Pegyhambarian, "Holmium-doped ZBLAN fiber lasers at 1.2 μm," Proc. SPIE **8237**, 823727 (2012).
79. X. Zhu, J. Zong, A. Miller, K. Wiersma, R. A. Norwood, N. S. Prasad, A. Chavez-Pirson, and N. Peyghambarian, "Single-frequency Ho^{3+}-doped ZBLAN fiber laser at 1200 nm," Opt. Lett. **37**, 4185–4187 (2012).
80. D. Hudson, E. Magi, L. Gomes, and S. D. Jackson, "1 W diode-pumped tunable Ho^{3+}, Pr^{3+}-doped fluoride glass fibre laser," Electron. Lett. **47**, 985–986 (2011).
81. D. D. Hudson, R. J. Williams, M. J. Withford, and S. D. Jackson, "Single-frequency fiber laser operating at 2.9 μm," Opt. Lett. **38**, 2388–2390 (2013).
82. S. Jiang and J. Wang, "Method of angle fusion splicing silica fiber with low-temperature non-silica fiber," U.S. patent 6,705,771 (March 16, 2004).
83. J. Wang and W. Li, "Method of fusion splicing silica fiber with low-temperature multi-component glass fiber," U.S. patent 6,866,429 (March 15, 2005).
84. H. Li, J. Lousteau, W. N. MacPherson, X. Jiang, H. T. Bookey, J. S. Barton, A. Jha, and A. K. Kar, "Thermal sensitivity of tellurite and germanate optical fibers," Opt. Express **15**, 8857–8863 (2007).
85. N. Jovanovic, M. Åslund, A. Fuerbach, S. D. Jackson, G. D. Marshall, and M. J. Withford, "Narrow linewidth, 100 W cw Yb^{3+}-doped silica fiber laser with a point-by-point Bragg grating inscribed directly into the active core," Opt. Lett. **32**, 2804–2806 (2007).
86. S. D. Jackson, A. Sabella, and D. G. Lancaster, "Application and development of high-power and highly efficient silica-based fiber lasers operating at 2 μm," IEEE J. Sel. Top. Quantum Electron. **13**, 567–572 (2007).
87. J. Nilsson and D. N. Payne, "High-power fiber lasers," Science **332**, 921–922 (2011).
88. S. Fu, W. Shi, J. Lin, Q. Fang, Q. Sheng, H. Zhang, J. Wen, and J. Yao, "Single-frequency fiber laser at 1950 nm based on thulium-doped silica fiber," Opt. Lett. **40**, 5283–5286 (2015).
89. Q. Fang, W. Shi, X. Tian, B. Wang, J. Yao, and N. Peyghambarian, "978 nm single frequency actively-switched all fiber laser," IEEE Photon. Technol. Lett. **26**, 874–876 (2014).
90. W. Guan and J. R. Marciante, "A single-frequency, 2-cm, Yb-doped silica fiber laser," in *Frontiers in Optics*, OSA Technical Digest (Optical Society of America, 2006), paper JSuA57.
91. W. Shi, S. Fu, Q. Fang, Q. Sheng, H. Zhang, X. Bai, G. Shi, J. Li, and J. Yao, "Single-frequency fiber laser based on rare-earth-doped silica fiber," Infrared Laser Eng. **45**, 1003001 (2016).
92. Q. Fang, Y. Xu, S. Fu, and W. Shi, "Single-frequency distributed Bragg reflector Nd doped silica fiber laser at 930 nm," Opt. Lett. **41**, 1829–1832 (2016).
93. G. A. Ball, C. G. Hull-Allen, and J. Livas, "Frequency noise of a Bragg grating fibre," Electron. Lett. **30**, 1229–1230 (1994).
94. E. Rønnekleiv, "Frequency and intensity noise of single frequency fiber Bragg grating lasers," Opt. Fiber Technol. **7**, 206–235 (2001).
95. P. Horak, N. Y. Voo, M. Ibsen, and W. H. Loh, "Pump-noise-induced linewidth contributions in distributed feedback fiber lasers," IEEE Photon. Technol. Let. **18**, 998–1000 (2006).
96. S. B. Foster and A. E. Tikhomirov, "Pump-noise contribution to frequency noise and linewidth of distributed-feedback fiber lasers," IEEE J. Quantum Electron. **46**, 734–741 (2010).
97. G. Di Domenico, S. Schilt, and P. Thomann, "Simple approach to the relation between laser frequency noise and laser line shape," Appl. Opt. **49**, 4801–4807 (2010).
98. G. A. Ball, G. Hull-Allen, C. Holton, and W. W. Morey, "Low noise single frequency linear fibre laser," Electron. Lett. **29**, 1623–1625 (1993).
99. G. A. Ball, C. E. Holton, G. Hull-Allen, and W. W. Morey, "60 mW 1.5 μm single frequency low-noise fibre laser MOPA," IEEE Photon. Technol. Lett. **6**, 192–194 (1994).
100. S. Taccheo, G. D. Geronimo, P. Laporta, and O. Svelto, "Intensity noise reduction in a single-frequency ytterbium-codoped erbium laser," Opt. Lett. **21**, 1747–1749 (1996).
101. Y. Xiao, C. Li, S. Xu, Z. Feng, C. Yang, Q. Zhao, and Z. Yang, "Simultaneously suppressing low-frequency and relaxation oscillation intensity noise in a DBR single-frequency phosphate fiber laser," Chin. Phys. Lett. **32**, 064205 (2015).
102. C. Li, S. Xu, Y. Xiao, Z. Feng, C. Yang, K. Zhou, and Z. Yang, "Simultaneously reducing the intensity and frequency noise of single-frequency phosphate fiber laser," J. Opt. **17**, 075802 (2015).
103. A. Wang, H. Ming, F. Li, L. Xu, L. Lv, H. Gui, J. Huang, and J. Xie, "Single-frequency, single-polarization ytterbium-doped fiber laser by self-injection locking," Chin. Opt. Lett. **2**, 223–225 (2004).
104. Z. Q. Pan, J. Zhou, F. Yang, Q. Ye, H. W. Cai, R. H. Qu, and Z. J. Fang, "Low-frequency noise suppression of a fiber laser based on a round-trip EDFA power stabilizer," Laser Phys. **23**, 035105 (2013).
105. Y. L. Zhao, Q. P. Wang, J. Chang, J. S. Ni, C. Wang, Z. H. Sun, P. P. Wang, G. P. Lv, and G. D. Peng, "Suppression of the intensity noise in distributed feedback fiber lasers by self-injection locking," Laser Phys. Lett. **9**, 739–743 (2012).
106. Y. Hou, Q. Zhang, and P. Wang, "Frequency- and intensity-noise suppression in Yb^{3+}-doped single-frequency fiber laser by a passive optical-feedback loop," Opt. Express **24**, 12991–12999 (2016).
107. G. A. Cranch, "Frequency noise reduction in erbium-doped fiber distributed-feedback lasers by electronic feedback," Opt. Lett. **27**, 1114–1116 (2002).
108. C. Li, S. Xu, X. Huang, Y. Xiao, Z. Feng, C. Yang, K. Zhou, W. Lin, J. Gan, and Z. Yang, "All-optical frequency and intensity noise suppression of single-frequency fiber laser," Opt. Lett. **40**, 1964–1967 (2015).
109. M. Yamada, "Analysis of intensity and frequency noises in semiconductor optical amplifier," IEEE J. Quantum Electron. **48**, 980–990 (2012).
110. G. Danion, F. Bondu, G. Loas, and M. Alouini, "GHz bandwidth noise eater hybrid optical amplifier: design guidelines," Opt. Lett. **39**, 4239–4242 (2014).

111. Z. Feng, C. Li, S. Xu, X. Huang, C. Yang, K. Zhou, J. Gan, H. Deng, and Z. Yang, "Significant intensity noise suppression of single-frequency fiber laser via cascading semiconductor optical amplifier," Laser Phys. Lett. **12**, 095101 (2015).
112. A. D. McCoy, L. B. Fu, M. Ibsen, B. C. Thomsen, and D. J. Richardson, "Intensity noise suppression in fibre DFB laser using gain saturated SOA," Electron. Lett. **40**, 107–109 (2004).
113. Q. Zhao, S. Xu, K. Zhou, C. Yang, C. Li, Z. Feng, M. Peng, H. Deng, and Z. Yang, "Broad-bandwidth near-shot-noise-limited intensity noise suppression of a single-frequency fiber laser," Opt. Lett. **41**, 1333–1335 (2016).
114. S. Mo, Z. Li, X. Huang, S. Xu, Z. Feng, W. Zhang, C. Li, C. Yang, Q. Qian, and D. Chen, "820 Hz linewidth short-linear-cavity single-frequency fiber laser at 1.5 μm," Laser Phys. Lett. **11**, 35101 (2014).
115. S. Mo, X. Huang, S. Xu, Z. Feng, C. Li, C. Yang, and Z. Yang, "Compact slow-light single-frequency fiber laser at 1550 nm," Appl. Phys. Express **8**, 082703 (2015).
116. S. Mo, X. Huang, S. Xu, C. Li, C. Yang, Z. Feng, W. Zhang, D. Chen, and Z. Yang, "600-Hz linewidth short-linear-cavity fiber laser," Opt. Lett. **39**, 5818–5821 (2014).
117. T. Zhu, X. Bao, L. Chen, H. Liang, and Y. Dong, "Experimental study on stimulated Rayleigh scattering in optical fibers," Opt. Express **18**, 22958–22963 (2010).
118. T. Zhu, S. Huang, L. Shi, W. Huang, M. Liu, and K. Chiang, "Rayleigh backscattering: a method to highly compress laser linewidth," Chin. Sci. Bull. **59**(33), 4631–4636 (2014).
119. G. Yin, B. Saxena, and X. Bao, "Tunable Er-doped fiber ring laser with single longitudinal mode operation based on Rayleigh backscattering in single mode fiber," Opt. Express **19**, 25981–25989 (2011).
120. G. P. Agrawal, *Nonlinear Fiber Optics* (Academic, 2007).
121. T. Zhu, X. Bao, and L. Chen, "A single longitudinal-mode tunable fiber ring laser based on stimulated Rayleigh scattering in a nonuniform optical fiber," J. Lightwave Technol. **29**, 1802–1807 (2011).
122. T. Zhu, F. Y. Chen, S. H. Huang, and X. Y. Bao, "An ultra-narrow linewidth fiber laser based on Rayleigh backscattering in a tapered optical fiber," Laser Phys. Lett. **10**, 055110 (2013).
123. T. Zhu, B. Zhang, L. Shi, S. Huang, M. Deng, J. Liu, and X. Li, "Tunable dual-wavelength fiber laser with ultra-narrow linewidth based on Rayleigh backscattering," Opt. Express **24**, 1324–1330 (2016).
124. X. Wang, Y. Yang, M. Liu, and Y. Yao, "Tunable multiwavelength narrow linewidth Brillouin erbium fiber laser based on Rayleigh backscattering," Opt. Eng. **55**, 066106 (2016).
125. P. Dainese, P. St. J. Russell, N. Joly, J. C. Knight, G. S. Wiederhecker, H. L. Fragnito, V. Laude, and A. Khelif, "Stimulated Brillouin scattering from multi-GHz-guided acoustic phonons in nanostructured photonic crystal fibres," Nat. Phys. **2**, 388–392 (2006).
126. W. Shi, Q. Fang, X. Zhu, R. A. Norwood, and N. Peyghambarian, "Fiber lasers and their applications [Invited]," Appl. Opt. **53**, 6554–6568 (2014).
127. A. Kobyakov, M. Sauer, and D. Chowdhury, "Stimulated Brillouin scattering in optical fibers," Adv. Opt. Photon. **2**, 1 (2010).
128. A. Debut, S. Randoux, and J. Zemmouri, "Linewidth narrowing in Brillouin lasers: theoretical analysis," Phys. Rev. A **62**, 023803 (2000).
129. A. Debut, S. Randoux, and J. Zemmouri, "Experimental and theoretical study of linewidth narrowing in Brillouin fiber ring lasers," J. Opt. Soc. Am. B **18**, 556–567 (2001).
130. S. P. Smith, F. Zarinetchi, and S. Ezekiel, "Narrow-linewidth stimulated Brillouin fiber laser and applications," Opt. Lett. **16**, 393–395 (1991).
131. M. Chen, Z. Meng, J. Wang, and W. Chen, "Strong linewidth reduction by compact Brillouin/erbium fiber laser," IEEE Photon. J. **6**, 1–8 (2014).
132. L. F. Stokes, M. Chodorow, and H. J. Shaw, "All-fiber stimulated Brillouin ring laser with submilliwatt pump threshold," Opt. Lett. **7**, 509–511 (1982).
133. G. Wang, L. Zhan, J. Liu, T. Zhang, J. Li, L. Zhang, J. Peng, and L. Yi, "Watt-level ultrahigh-optical signal-to-noise ratio single-longitudinal-mode tunable Brillouin fiber laser," Opt. Lett. **38**, 19–21 (2013).
134. Y. Luo, Y. Tang, J. Yang, Y. Wang, S. Wang, K. Tao, L. Zhan, and J. Xu, "High signal-to-noise ratio, single-frequency 2 μm Brillouin fiber laser," Opt. Lett. **39**, 2626–2628 (2014).
135. G. J. Cowle and D. Y. Stepanov, "Hybrid Brillouin/erbium fiber laser," Opt. Lett. **21**, 1250–1252 (1996).
136. W. Guan and J. R. Marciante, "Single-frequency 1 W hybrid Brillouin/ytterbium fiber laser," Opt. Lett. **34**, 3131–3132 (2009).
137. D. Y. Stepanov and J. C. Gregory, "Properties of Brillouin/erbium fiber lasers," IEEE J. Sel. Top. Quantum Electron. **3**, 1049–1057 (1997).
138. S. W. Harun, S. Shahi, and H. Ahmad, "Compact Brillouin-erbium fiber laser," Opt. Lett. **34**, 46–48 (2009).
139. M. Chen, Z. Meng, and H. Zhou, "Low-threshold, single-mode, compact Brillouin/erbium fiber ring laser," J. Lightwave Technol. **31**, 1980–1986 (2013).
140. M. Chen, Z. Meng, Y. Zhang, J. Wang, and W. Chen, "Ultranarrow-linewidth Brillouin/erbium fiber laser based on 45-cm erbium-doped fiber," IEEE Photon. J. **7**, 1–6 (2015).
141. Y. Shen, Y. Qiu, B. Wu, W. Zhao, S. Chen, T. Sun, and K. T. V. Grattan, "Short cavity single frequency fiber laser for in-situ sensing applications over a wide temperature range," Opt. Express **15**, 363–370 (2007).
142. S. Mo, S. Xu, X. Huang, W. Zhang, Z. Feng, D. Chen, T. Yang, and Z. Yang, "A 1014 nm linearly polarized low noise narrow-linewidth single-frequency fiber laser," Opt. Express **21**, 12419–12423 (2013).
143. K. N. Choi and H. F. Taylor, "Spectrally stable Er-fiber laser for application in phase-sensitive optical time-domain reflectometry," IEEE Photon. Technol. Lett. **15**, 386–388 (2003).
144. W. Liang, V. S. Ilchenko, A. A. Savchenkov, A. B. Matsko, D. Seidel, and L. Maleki, "Whispering-gallery-mode-resonator-based ultranarrow linewidth external-cavity semiconductor laser," Opt. Lett. **35**, 2822–2824 (2010).
145. D. K. Shin, B. M. Henson, R. I. Khakimov, J. A. Ross, C. J. Dedman, S. S. Hodgman, K. G. H. Baldwin, and A. G. Truscott, "Widely tunable, narrow linewidth external-cavity gain chip laser for spectroscopy between 1.0–1.1 μm," Opt. Express **24**, 27403–27414 (2016).
146. A. Liu, "Stimulated Brillouin scattering in single-frequency fiber amplifiers with delivery fibers," Opt. Express **17**, 15201–15209 (2009).
147. D. P. Machewirth, Q. Wang, B. Samson, K. Tankala, M. O'Connor, and M. Alam, "Current developments in high-power monolithic polarization maintaining fiber amplifiers for coherent beam combining applications," Proc. SPIE **6453**, 64531F (2007).
148. M. D. Mermelstein, K. Brar, M. J. Andrejco, A. D. Yablon, M. Fishteyn, C. Headley III, and D. J. DiGiovanni, "All-fiber 194 W single-frequency single-mode Yb-doped master-oscillator power-amplifier," Proc. SPIE **6873**, 68730L (2008).
149. P. Ma, P. Zhou, Y. Ma, R. Su, X. Xu, and Z. Liu, "Single-frequency 332 W, linearly polarized Yb-doped all-fiber amplifier with near diffraction-limited beam quality," Appl. Opt. **52**, 4854–4857 (2013).
150. L. Huang, H. Wu, R. Li, L. Li, P. Ma, X. Wang, J. Leng, and P. Zhou, "414 W near-diffraction-limited all-fiberized single-frequency polarization- maintained fiber amplifier," Opt. Lett. **42**, 1–4 (2017).
151. C. Zeringue, C. Vergien, and I. Dajani, "Pump-limited, 203 W, single-frequency monolithic fiber amplifier based on laser gain competition," Opt. Lett. **36**, 618–620 (2011).
152. C. Robin, I. Dajani, and B. Pulford, "Modal instability-suppressing, single-frequency photonic crystal fiber amplifier with 811 W output power," Opt. Lett. **39**, 666–669 (2014).
153. T. Theeg, C. Ottenhues, H. Sayinc, J. Neumann, and D. Kracht, "Core-pumped single-frequency fiber amplifier with an output power of 158 W," Opt. Lett. **41**, 9–12 (2016).
154. L. Wei, F. Cleva, and C. N. Man, "Coherently combined master oscillator fiber power amplifiers for Advanced Virgo," Opt. Lett. **41**, 5817–5820 (2016).
155. B. G. Ward, "Maximizing power output from continuous-wave single-frequency fiber amplifiers," Opt. Lett. **40**, 542–545 (2015).
156. B. Pulford, T. Ehrenreich, R. Holten, F. Kong, T. W. Hawkins, L. Dong, and I. Dajani, "400-W near diffraction-limited single-frequency all-solid photonic bandgap fiber amplifier," Opt. Lett. **40**, 2297–2300 (2015).
157. J. Zhu, P. Zhou, X. Wang, X. Xu, and Z. Liu, "Analysis of maximum extractable power of single-frequency-doped phosphate fiber sources," IEEE J. Quantum Electron. **48**, 480–484 (2012).
158. M. Dubinskii and V. V. Ter-Mikirtychev, "Scalable, single-frequency, Er-only doped fiber amplifier cladding-pumped by multimode 980-nm

diode lasers," in *Advanced Solid-State Photonics*, OSA Technical Digest Series (Optical Society of America, 2008), paper WE24.
159. Y. Jeong, J. K. Sahu, D. B. S. Soh, C. A. Codemard, and J. Nilsson, "High-power tunable single-frequency single-mode erbium:ytterbium codoped large-core fiber master-oscillator power amplifier source," Opt. Lett. **30**, 2997–2999 (2005).
160. C. Yang, S. Xu, S. Mo, C. Li, Z. Feng, D. Chen, Z. Yang, and Z. Jiang, "10.9 W kHz-linewidth one-stage all-fiber linearly-polarized MOPA laser at 1560 nm," Opt. Express **21**, 12546–12551 (2013).
161. M. Steinke, A. Croteau, C. Paré, H. Zheng, P. Laperle, A. Proulx, J. Neumann, D. Kracht, and P. Wessels, "Co-seeded Er^{3+}:Yb^{3+} single frequency fiber amplifier with 60 W output power and over 90% TEM00 content," Opt. Express **22**, 16722–16730 (2014).
162. X. Bai, Q. Sheng, H. Zhang, S. Fu, W. Shi, and J. Yao, "High-power all-fiber single-frequency erbium–ytterbium co-doped fiber master oscillator power amplifier," IEEE Photon. J. **7**, 1–10 (2015).
163. D. Creeden, H. Pretorius, J. Limongelli, and S. D. Setzler, "Single frequency 1560 nm Er:Yb fiber amplifier with 207 W output power and 50.5% slope efficiency," Proc. SPIE **9728**, 97282L (2016).
164. D. Gapontsev, N. Platonov, M. Meleshkevich, O. Mishechkin, O. Shkurikhin, S. Agger, P. Varming, and J. H. Povlsen, "20 W single-frequency fiber laser operating at 1.93 μm," in *Conference on Lasers and Electro-Optics/Quantum Electronics and Laser Science Conference and Photonic Applications Systems Technologies*, OSA Technical Digest Series (Optical Society of America, 2007), paper CFI5.
165. G. D. Goodno, L. D. Book, and J. E. Rothenberg, "Low-phase-noise, single-frequency, single-mode 608 W thulium fiber amplifier," Opt. Lett. **34**, 1204–1206 (2009).
166. X. Wang, P. Zhou, X. Wang, H. Xiao, and L. Si, "102 W monolithic single frequency Tm-doped fiber MOPA," Opt. Express **21**, 32386–32392 (2013).
167. J. Liu, H. Shi, K. Liu, Y. Hou, and P. Wang, "210 W single-frequency, single-polarization, thulium-doped all-fiber MOPA," Opt. Express **22**, 13572–13578 (2014).
168. L. Li, B. Zhang, K. Yin, and J. Hou, "75 W single-frequency, thulium-doped fiber laser at 2.05 μm," Laser Phys. Lett. **12**, 095103 (2015).
169. X. Wan, X. Jin, W. Wu, P. Zhou, X. Wang, H. Xiao, and Z. Liu, "310-W single frequency Tm-doped all-fiber MOPA," IEEE Photon. Technol. Lett. **27**, 677–680 (2015).
170. C. Yang, D. Chen, S. Xu, H. Deng, W. Lin, Q. Zhao, Y. Zhang, K. Zhou, Z. Feng, Q. Qian, and Z. Yang, "Short all Tm-doped germanate glass fiber MOPA single-frequency laser at 1.95 μm," Opt. Express **24**, 10956–10961 (2016).
171. E. M. Dianov, "Advances in Raman fibers," J. Lightwave Technol. **20**, 1457–1462 (2002).
172. C. Robin and I. Dajani, "Acoustically segmented photonic crystal fiber for single-frequency high-power laser applications," Opt. Lett. **36**, 2641–2643 (2011).
173. I. Dajani, C. Vergien, C. Robin, and B. Ward, "Investigations of single-frequency Raman fiber amplifiers operating at 1178 nm," Opt. Express **21**, 12038–12052 (2013).
174. C. Vergien, I. Dajani, and C. Robin, "18 W single-stage single-frequency acoustically tailored Raman fiber amplifier," Opt. Lett. **37**, 1766–1768 (2012).
175. L. Zhang, J. Hu, J. Wang, and Y. Feng, "Stimulated-Brillouin-scattering-suppressed high-power single-frequency polarization-maintaining Raman fiber amplifier with longitudinally varied strain for laser guide star," Opt. Lett. **37**, 4796–4798 (2012).
176. L. Zhang, H. Jiang, S. Cui, J. Hu, and Y. Feng, "Versatile Raman fiber laser for sodium laser guide star," Laser Photon. Rev. **8**, 889–895 (2014).
177. W. Renard, T. Robin, B. Cadier, J. Le Gouët, L. Lombard, A. Durécu, P. Bourdon, and G. Canat, "High peak power single-frequency efficient erbium–ytterbium doped LMA fiber," in *CLEO: 2015*, OSA Technical Digest (Optical Society of America, 2015), paper STh4L.6.
178. L. V. Kotov, M. E. Likhachev, M. M. Bubnov, V. M. Paramonov, M. I. Belovolov, D. S. Lipatov, and A. N. Guryanov, "Record-peak-power all-fiber single-frequency 1550 nm laser," Laser Phys. Lett. **11**, 095102 (2014).
179. W. Shi, E. B. Petersen, M. Leigh, J. Zong, Z. Yao, A. Chavez-Pirson, and N. Peyghambarian, "High SBS-threshold single-mode single-frequency monolithic pulsed fiber laser in the C-band," Opt. Express **17**, 8237–8245 (2009).
180. W. Shi, E. B. Petersen, Z. Yao, D. T. Nguyen, J. Zong, M. A. Stephen, A. Chavez-Pirson, and N. Peyghambarian, "Kilowatt-level stimulated-Brillouin-scattering-threshold monolithic transform-limited 100 ns pulsed fiber laser at 1530 nm," Opt. Lett. **35**, 2418–2420 (2010).
181. W. Shi, E. B. Petersen, D. T. Nguyen, Z. Yao, A. Chavez-Pirson, N. Peyghambarian, and J. Yu, "220 μJ monolithic single-frequency *Q*-switched fiber laser at 2 μm by using highly Tm-doped germanate fibers," Opt. Lett. **36**, 3575–3577 (2011).
182. Q. Fang, W. Shi, E. Petersen, K. Kieu, A. Chavez-Pirson, and N. Peyghambarian, "Half-mJ all-fiber-based single-frequency nanosecond pulsed fiber laser at 2 μm," IEEE Photon. Technol. Lett. **24**, 353–355 (2012).
183. Q. Fang, W. Shi, K. Kieu, E. Petersen, A. Chavez-Pirson, and N. Peyghambarian, "High power and high energy monolithic single frequency 2 μm nanosecond pulsed fiber laser by using large core Tm-doped germanate fibers: experiment and modeling," Opt. Express **20**, 16410–16420 (2012).
184. V. I. Kovalev and R. G. Harrison, "Suppression of stimulated Brillouin scattering in high-power single-frequency fiber amplifiers," Opt. Lett. **31**, 161–163 (2006).
185. N. Yoshizawa and T. Imai, "Stimulated Brillouin scattering suppression by means of applying strain distribution to fiber with cabling," J. Lightwave Technol. **11**, 1518–1522 (1993).
186. J. M. C. Boggio, J. D. Marconi, and H. L. Fragnito, "Experimental and numerical investigation of the SBS-threshold increase in an optical fiber by applying strain distributions," J. Lightwave Technol. **23**, 3808–3814 (2005).
187. Z. Ren, J. Wang, J. Zhou, J. Liu, and W. Chen, "Single-frequency high-energy Yb-doped pulsed all-fiber laser," Chin. Opt. Lett. **10**, 091402 (2012).
188. X. Zhang, W. Diao, Y. Liu, X. Zhu, Y. Yang, J. Liu, X. Hou, and W. Chen, "Eye-safe single-frequency single-mode polarized all-fiber pulsed laser with peak power of 361 W," Appl. Opt. **53**, 2465–2469 (2014).
189. R. Su, P. Zhou, H. Xiao, X. Wang, and X. Xu, "150 W high-average-power, single-frequency nanosecond fiber laser in strictly all-fiber format," Appl. Opt. **51**, 3655–3659 (2012).
190. R. Su, P. Zhou, P. Ma, H. Lü, and X. Xu, "High-peak-power, single-frequency, single-mode, linearly polarized, nanosecond all-fiber laser based on self-phase modulation compensation," Appl. Opt. **52**, 7331–7335 (2013).
191. X. Wang, P. Zhou, R. Su, H. Xiao, X. Xu, and Z. Liu, "A 280 W high average power, single-frequency all-fiber nanosecond pulsed laser," Laser Phys. **23**, 015101 (2012).
192. R. T. Su, X. L. Wang, P. Zhou, and X. J. Xu, "All-fiberized master oscillator power amplifier structured narrow-linewidth nanosecond pulsed laser with 505 W average power," Laser Phys. Lett. **10**, 015105 (2012).
193. R. Su, P. Zhou, X. Wang, Y. Ma, H. Xiao, P. Ma, X. Xu, and Z. Liu, "High power narrow-linewidth nanosecond all-fiber lasers and their actively coherent beam combination," IEEE J. Sel. Top. Quantum Electron. **20**, 206–218 (2014).
194. M. Leigh, W. Shi, J. Zong, Z. Yao, S. Jiang, and N. Peyghambarian, "High peak power single frequency pulses using a short polarization-maintaining phosphate glass fiber with a large core," Appl. Phys. Lett. **92**, 181108 (2008).
195. E. Petersen, W. Shi, A. Chavez-Pirson, and N. Peyghambarian, "High peak-power single-frequency pulses using multiple stage, large core phosphate fibers and preshaped pulses," Appl. Opt. **51**, 531–534 (2012).
196. J. Geng, Q. Wang, Z. Jiang, T. Luo, S. Jiang, and G. Czarnecki, "Kilowatt-peak-power, single-frequency, pulsed fiber laser near 2 μm," Opt. Lett. **36**, 2293–2295 (2011).